Ocean Engineering 82 (2014) 75–84

Contents lists available at ScienceDirect

Ocean Engineering

journal homepage: www.elsevier.com/locate/oceaneng

Experimental study on sloshing in a tank with an inner horizontal perforated plate

Heng Jin, Yong Liu*, Hua-Jun Li

Shandong Provincial Key Laboratory of Ocean Engineering, Ocean University of China, Qingdao 266100, China

ARTICLE INFO

Article history:
Received 14 October 2013
Accepted 22 February 2014
Available online 15 March 2014

Keywords:
Horizontal perforated plate
Sloshing
Resonant frequency
Experimental test
Surface elevation

ABSTRACT

Sloshing in a liquid tank may result in ship instability or structural damage. Inner structures are often used to restrain liquid sloshing and prevent tank damage. To increase energy dissipation and reduce the forces acting on structures, a horizontal perforated plate was designed and incorporated into a rectangular liquid tank in this study. Experimental studies were conducted, and a tank with an inner submerged horizontal perforated plate was excited under different amplitudes and frequencies. The free surface elevations on the side-walls and the resonant frequencies were carefully examined. The experimental results indicate that the horizontal perforated plate can significantly restrain violent resonant sloshing in the tank under horizontal excitation.

1. Introduction

Sloshing occurs in a moving tank containing liquid with a free surface and may result in the resonant excitation of the tank liquid. A partially filled ship tank may experience violent liquid motion when the ship motion involves energy in the vicinity of the natural frequency of the liquid motion inside the tank. This liquid motion was of primary practical interest in this study.

Many studies with respect to sloshing focus on methods for suppressing resonant sloshing and reducing sloshing loads. Baffles and perforated plates are efficient inner structures for suppressing resonant sloshing. Their applicability has been confirmed over the last century for liquid sloshing in fuel rocket tanks (Abramson, 1966). Swash bulkheads (vertical baffles) in cargo ship liquid tanks are also useful for restraining sloshing. The functions of swash bulkheads are to provide sloshing damping and to promote the lowest resonant frequency to a higher frequency range over which the wave-induced ship velocity and acceleration are less severe. Rectangular tanks with perforated vertical plates are used for the anti-rolling tanks of ships and tuned liquid dampers (TLDs) of tall buildings. Properly tuned sloshing is an efficient tool for suppressing oscillations of carrying structures. For this application, the lowest resonant sloshing frequency should remain nearly by the inner structures.

Previous attempts to make accurate predictions of the sloshing-induced dynamic pressures on the inner structures and walls of fuel tanks were made by Abramson (1966). A further analytical study on the effects of a vertical baffle on the resonant frequencies of fluid in a rectangular tank was performed by Evans and McIver (1987). The authors observed that a surface-piercing barrier changed the resonant frequencies significantly, whereas the effect of a bottom-mounted barrier was negligible. Recently, Akyildiz (2012) and Jung et al. (2012) observed that increasing the heights of vertical baffles may enhance liquid sloshing suppression, and Goudarzi and Sabbagh-Yazdi (2012) showed that an up-mounted vertical baffle is more effective than a low-mounted one. The use of vertical baffles may not only remarkably reduce the natural frequency of liquid storage tank systems but also reduce the sloshing amplitude and dynamic impact loads acting on tank walls (Armenio and Rocca, 1996; Wu et al., 2013; Xue et al., 2012). In addition to vertical baffles, alternative structures have been incorporated into tanks, such as annular baffles and flexible baffles in cylindrical tanks (Biswal et al., 2004), horizontal baffles in cubic tanks (Akyildiz and Unal, 2005, 2006; Liu and Lin, 2009) and annular baffles in rectangular tanks (Panigrahy et al., 2009). Among these inner structures, annular baffles proved most efficient.

The forces acting on structures inside a water tank due to resonant sloshing may be relatively large. These large forces can be significantly reduced by perforating the inner structures. In addition, a perforated inner structure may dissipate more of the energy of the sloshing fluid. Perforated inner structures have garnered some attention among researchers. Tait et al. (2005a) investigated a tuned liquid damper (TLD) equipped with vertical perforated screens under 2D excitation. Their experimental results showed that perforated screens work well as an inner structure in TLDs. More recently, Tait et al. (2005b) developed two numerical models to simulate the linear and non-linear effects of sloshing. The linear

* Corresponding author. Tel.: +86 532 66781129; fax: +86 532 66781550.
E-mail address: liuyong_77@hotmail.com (Y. Liu).

http://dx.doi.org/10.1016/j.oceaneng.2014.02.024
0029-8018

model was capable of providing a preliminary design for the size, number and position of a TLD slat screen. However, more detailed TLD response characteristics should be analyzed using the non-linear model. Dodge (2000) experimentally demonstrated that the porosity of the inner baffle influences the slosh dynamics, but a change in the natural frequency requires a porosity of 10% or less. Recently, Faltinsen and his collaborators (Faltinsen et al., 2010, 2011; Faltinsen and Timokha, 2011) conducted detailed studies on liquid motions in a rectangular tank with a vertical slat-type screen in the middle of the tank. The authors observed that the resonant frequency of the tank with a screen was different from the natural frequency of a clean tank. They also observed that the resonant sloshing frequencies depend on the solidity ratio (unity minus the porosity), the number of submerged screen gaps, the liquid depth, and the position of the perforated openings relative to the mean free surface. The resonant frequency monotonically decreased as the solidity ratio increased. The largest amplitude response was at the resonant frequency corresponding to the third-order natural frequency of the clean tank, because the first mode disappeared and the third mode decreased. Cassolato et al. (2011) experimentally studied a TLD with inclined slat screens and observed that the energy loss coefficient of a screen decreased with an increase in the angle of inclination, and the screen had a negligible effect on the natural frequency of the water tank.

In addition to aforementioned vertical baffles and screens, horizontal plates have also been installed in water tanks to suppress sloshing. Kim (2001) proved that a horizontal plate reduces the impulsive pressure on a tank ceiling. Cho et al. (2005) and Biswal et al. (2006) demonstrated that decreasing the submerged depth or increasing the width of a horizontal plate is helpful in reducing the maximum sloshing wave heights. Isaacson and Premasiri (2001) compared horizontal and vertical inner plates and observed that horizontal plates are more effective in damping liquid motion in deeper tanks, whereas vertical plates are better for shallower water tanks. Goudarzi and Sabbagh-Yazdi (2012) further observed that horizontal plates exhibit significant damping effects in slender tanks, whereas vertical plates are more effective in broader tanks. In addition to their applications in sloshing tanks, horizontal plates have been proposed as an efficient offshore breakwater in coastal engineering (Yu, 2002). An adequately designed horizontal perforated plate breakwater may exhibit significant wave-absorbing performance and reduce wave forces (Yu and Chwang, 1994; Liu et al., 2007; Liu and Li, 2011). Evans and McIver (1987) found that a surface-piercing vertical barrier can suppress the sloshing better than a bottom one. The free surface movement might also be restrained well by a horizontal plate near the free surface. Thus, we may install a horizontal perforated plate inside a water tank to restrict fluid sloshing, which has been scarcely mentioned in the literature.

The primary objective of this study was to experimentally examine the effect of a horizontal perforated plate on fluid sloshing in a water tank. The experimental setup is introduced in the following section. In Section 3, the free surface elevations at the tank wall with different horizontal excitations and the changes after placing perforated plates in the tank are carefully examined. The effects of the porosity and the relative submerged depth of the horizontal plate on the resonant wave heights and resonant frequencies are demonstrated. Several useful results are presented for practical applications. Finally, the primary conclusions of this study are drawn.

2. Experimental setup

In this section, we provide a description of the experimental setup, including the water tank, vibrostand, vibration control system and wave probes. A Plexiglas rectangular tank (1.0 m length, 0.8 m height and 0.11 m breadth) was installed on a stable vibrostand. The tank was similar to that of Faltinsen et al. (2011). The factor determining our choice of tank breadth is that we wanted to achieve two-dimensional flow conditions, and hence, the breadth-to-length ratio had to be small. The tank was designed with an inner horizontal perforated plate, and the position of the inner plate could be changed (see Fig. 1). For testing the efficiency of the horizontal perforated plate and simplifying our experiment, the problem was restricted to liquid sloshing in a rectangular tank under sway oscillations $X(t) = A \sin(\omega t)$, where A and ω are the amplitude and angular frequency of excitation, respectively. The motion of the partially filled water tank was controlled by a servo motor and an eccentric wheel, as shown in Fig. 2. With different eccentric distances and voltages, different excitation amplitudes and frequencies could be achieved.

In our tests, the horizontal plate with perforated slots was mounted in the tank with different submerged depths. The configuration of the horizontal plate is shown in Fig. 1. The submerged depth of the plate (the space between the still water level and the plate) is a, and the distance between the horizontal plate and the tank bottom is h. The water depth is D, and $D = a + h$. For examining the effect of plate submerged depth, three different relative submerged depths of $a/D = 1/3$, $1/2$ and $2/3$ were used in the tests. The consideration wanted to detect a more effective plate configuration for damping violent sloshing. A geometrical sketch

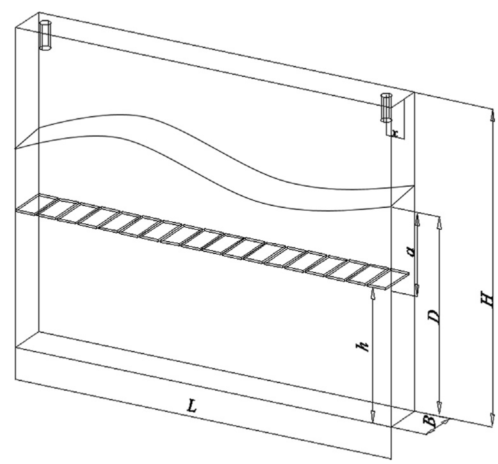

Fig. 1. Sketch of a rectangular tank with an inner horizontal perforated plate.

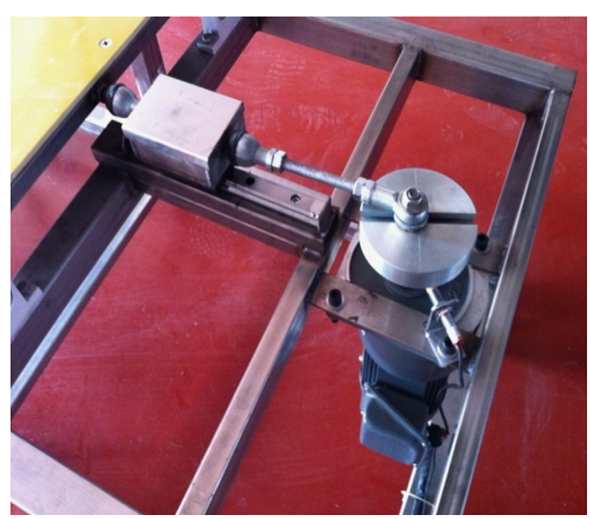

Fig. 2. Excitation device for the vibrostand.

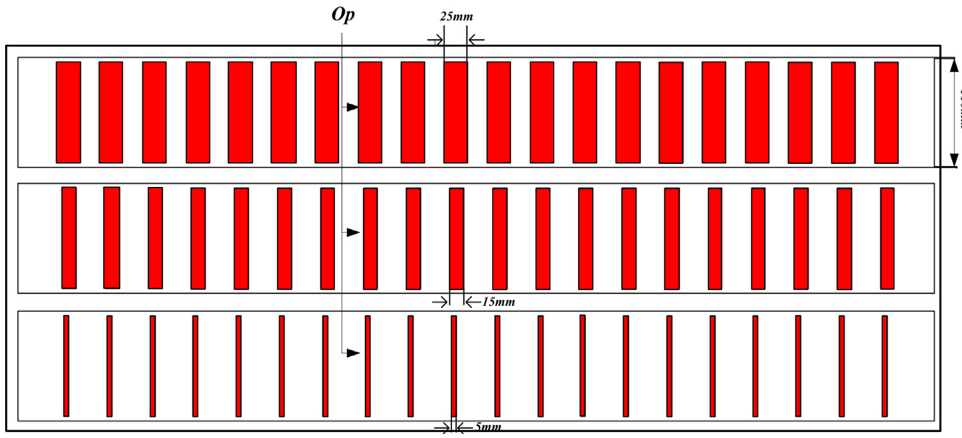

Fig. 3. Sketch of three different horizontal perforated plates used in the tests. (For interpretation of the references to color in this figure legend, the reader is referred to the web version of this article.)

of the perforated plates is illustrated in Fig. 3. The geometrical porosity P is defined as

$$P = \frac{n \times Op}{L}, \quad (Op = 5\text{ mm},\ 15\text{ mm},\ 25\text{ mm},\ n = 20), \tag{1}$$

where Op (red shadow in Fig. 3) is the width of the slot, n is the number of slots. Twenty slots were drilled on each horizontal plate. There were two limiting cases associated with $P=0$ (no plate) and $P=1$ (solid plate). To allow water to cross vertical porous plate and to offer greater damping to restrain non-linear sloshing, P should not exceed 10% (Dodge, 2000). Here we adopted three different porosities (including Dodge's value of $P=0.1$) to check the effect of porosity. Therefore, three P values of 0.5, 0.3 and 0.1 were used in the tests to study the effect of plate porosity on sloshing motion. The horizontal plate thickness was 5 mm, and the thickness effect could be neglected in the analysis (Faltinsen et al., 2011).

The tank natural frequencies are calculated according to Lamb (1932):

$$\omega_i = \sqrt{g\frac{\pi i}{L}\tanh\left(\frac{\pi i}{L}D\right)} \quad i = 1, 2, 3, \ldots \tag{2}$$

where ω_i is the natural frequency, and g is gravitational acceleration. The lowest linear mode ω_1 is of primary importance for the tank sloshing phenomenon. However, according to Faltinsen et al. (2011), adding a vertical perforated plate to a water tank may remove the first-order resonant frequency, and the third-order resonant frequency will change accordingly and become more dominant. Thus, the non-dimensional first-order mode ($\omega_1/\omega_1=1$) and third-order mode ($\omega_3/\omega_1=1.81$) were both considered when studying the resonant effect of sloshing under anti-symmetry movement in the present study. The excitation amplitudes used in the tests were $A=2.5$ mm and 8 mm to demonstrate the effects of the excitation amplitude on liquid sloshing. Before the tests, the excitation amplitudes and frequencies were verified using a highly accurate laser displacement sensor. The results showed that the excitation amplitudes were constant and accurate and that the frequencies were also steady, as shown in Fig. 4.

The tank was equipped with two resistant wave probes. The two probes were located 1.5 cm from the two opposite vertical walls (see Fig. 1). Both probes were calibrated before use. The time series of free surface elevations were recorded by a computer at a sample rate of 20 Hz over 40 s. Each test was repeated at least 3 times to check the precision of the results. For all tests, the water temperature was kept at 10.5 ± 0.5 °C, and the effect of the temperature was ignored.

Twenty cases involving different excitation amplitudes and relative submerged depths and porosities of the horizontal plates were examined. All of the experimental cases are listed in Table 1. The cases 1 – 1 and 1 – 2 represent a clean tank without an inner plate. In each case, the range of excitation frequencies was approximately 0.4–1.7 Hz, which covered the three lowest resonant frequencies for the clean tank with a liquid depth $D=0.5$ m. A total of 1560 test runs were performed in the experiments. D/L was set to 0.5 to avoid hydraulic jumps and other violent liquid motion. At this fill depth, the wave motion resembles a standing wave, with the largest free surface elevations appearing at the tank walls (Faltinsen and Timokha, 2009). This condition was convenient for capturing the data using wave probes located beside the side-walls.

3. Results with discussions

3.1. Time history of free surface elevations with small-amplitude excitation

In our tests, each excitation acting on the tank with a special frequency and amplitude was sustained for 40 s. The sloshing phenomenon for small-amplitude ($A/L=0.0025$) was studied first to obtain the characteristics of free surface elevations with a small nonlinear effect.

The free surface elevations measured by the two probes are anti-symmetric and the values are close. This can be observed in Fig. 5, where the comparison of the measured amplitudes of non-dimensional free surface elevation η_{max}/A at both side-walls (1.5 cm away) in the clean tank is shown. Thus, only the left wall data are presented in the next. To further verify our experiment, the analytical results of η_{max}/A at the side-walls of the clean tank are also added in Fig. 5. Here the analytical solution of η_{max}/A for a clean tank is calculated by (Linton and McIver, 2001; Eq. (2.37))

$$\frac{\eta_{max}}{A} = \frac{\omega}{gA}\left|A\omega b + \sum_{m=0}^{\infty}\frac{2K}{\mu_m^2 b(K_m - K)}\right|, \tag{3}$$

where, $b=L/2$, $\mu_m=(m+0.5)\pi/b$, $K_m=\mu_m \tanh \lambda_m D$, $K=\omega^2/g$. It can be seen from Fig. 5 that the agreement between experiments and predictions is reasonable.

Based on the time history of the free surface elevations at different excitation frequencies, a typical 3D time history of the free surface elevations is plotted in Fig. 6. The figure shows that the free surface elevation increases and reaches a steady state at approximately $\omega/\omega_1=1$ and 1.8. These frequencies are nearly the same as the natural frequencies ratios $\omega_1/\omega_1=1$ (first-order mode)

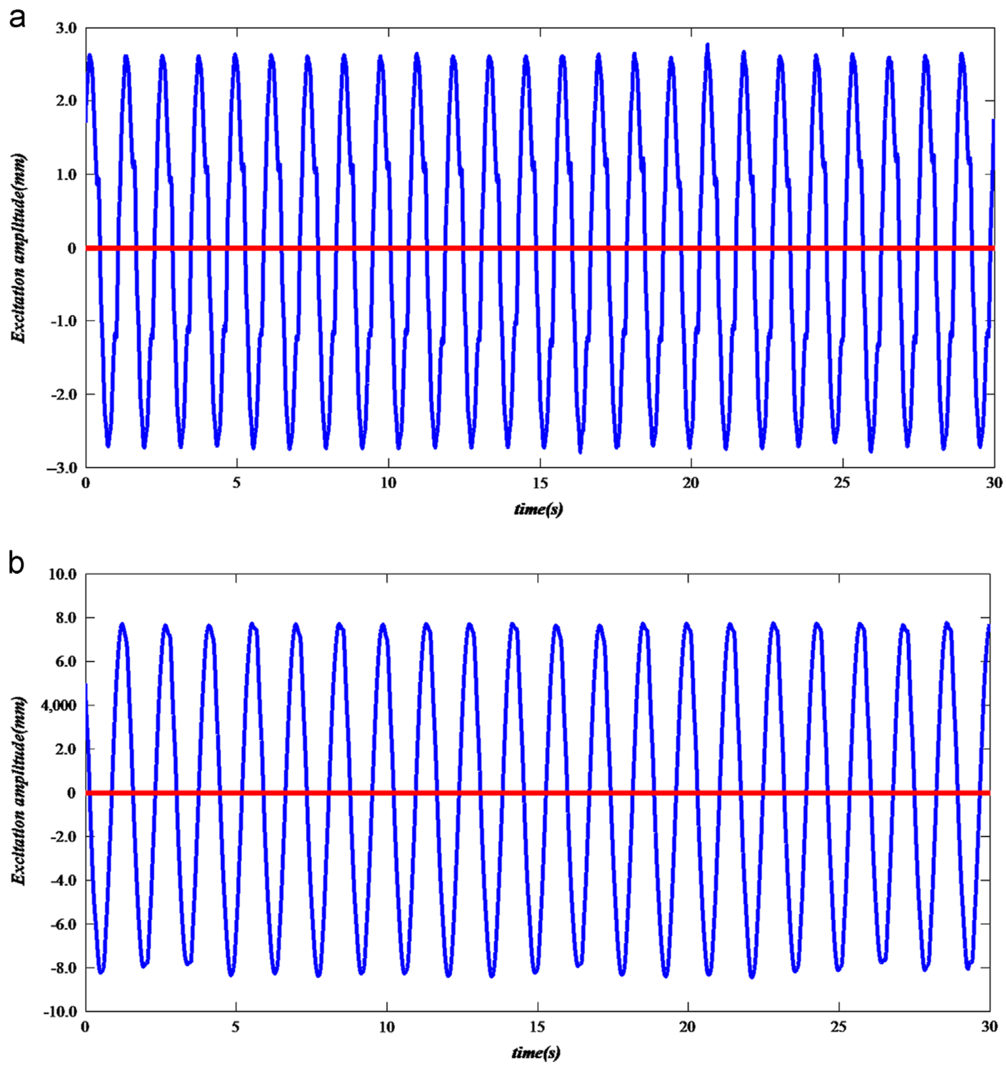

Fig. 4. (a) Validation of the excitation, amplitudes and frequencies, $A=2.5$ mm. (b) Validation of the excitation, amplitudes and frequencies, $A=8$ mm.

Table 1
Experimental cases examined in the model tests.

Cases	a/D	P	A/L	ω/ω_1	D/L
1 – 1	–	–	0.0025	0.5–2.0	0.5
2 – 1	2/3	0.5			
3 – 1	2/3	0.3			
4 – 1	2/3	0.1			
5 – 1	1/2	0.5			
6 – 1	1/2	0.3			
7 – 1	1/2	0.1			
8 – 1	1/3	0.5			
9 – 1	1/3	0.3			
10 – 1	1/3	0.1			
1 – 2	–	–	0.008	0.5–2.0	0.5
2 – 2	2/3	0.5			
3 – 2	2/3	0.3			
4 – 2	2/3	0.1			
5 – 2	1/2	0.5			
6 – 2	1/2	0.3			
7 – 2	1/2	0.1			
8 – 2	1/3	0.5			
9 – 2	1/3	0.3			
10 – 2	1/3	0.1			

and $\omega_3/\omega_1=1.81$ (third-order mode) for the clean tank without the inner horizontal plate. The largest free surface elevation occurs near the natural frequency. On the other hand, the free surface elevations at other frequencies are very small because there is no resonant effect. Fig. 6 also indicates that the horizontal plate with $a/D=2/3$ and $P=0.5$ (case 2 – 1) does not change the resonant frequency significantly. Because the large free surface elevations at the first-order and third-order resonant frequencies are several times the normal one, the resonant sloshing should be studied in detail to find a way to reduce the sloshing wave elevation or to remove the resonant effect.

Due to the large free surface elevations at the resonant frequency in case 2 – 1, the time history of the free surface elevations of other cases under the resonant frequency are plotted directly using the probe data. The data for cases 10 – 1, 4 – 1, 8 – 1 (small porosity or small relative submerged depth) and 1 – 1 (clean tank) are compared with the data for case 2 – 1 in Fig. 7.

As shown in Fig. 7, the results indicate that all four cases with the horizontal perforated plate can reduce the time required to reach the steady-state at the first-order mode. Thus, the maximum free surface elevation stops increasing at a low level. Resonant sloshing is restrained by the horizontal perforated plate. Among all cases, the free surface elevation at $a/D=1/3$, $P=0.1$ (case 10 – 1) is the lowest. Cases 4 – 1 and 8 – 1 show a similar effect on the resonant sloshing. This finding indicates that a special suppression effect could be achieved by adjusting either the location or porosity of the horizontal plate. Additionally, an unexpected increase appears in the first 15 s for case 2 – 1, as shown in Fig. 7. The free surface

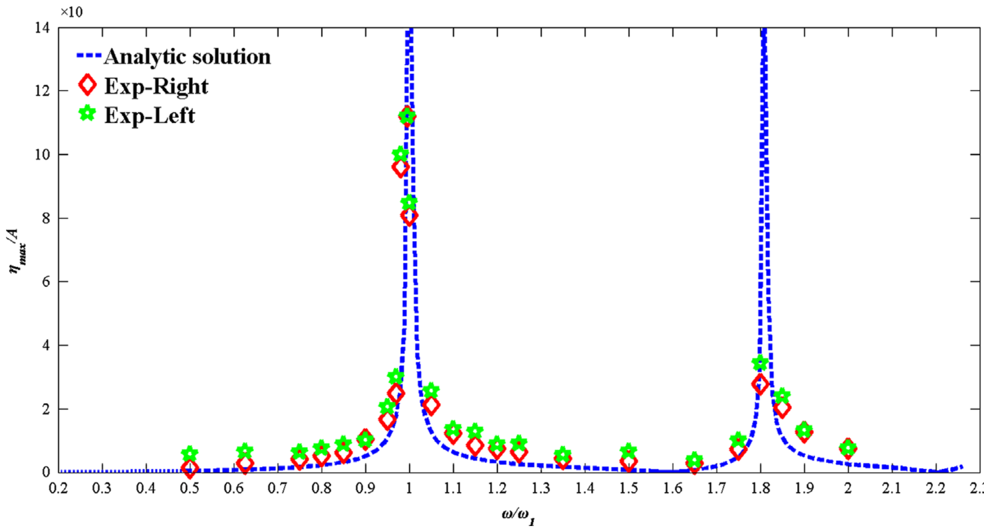

Fig. 5. Measured and predicted amplitudes of the non-dimensional free surface elevations at side-walls of clean tank at $A/L=0.0025$ and $D/L=0.5$.

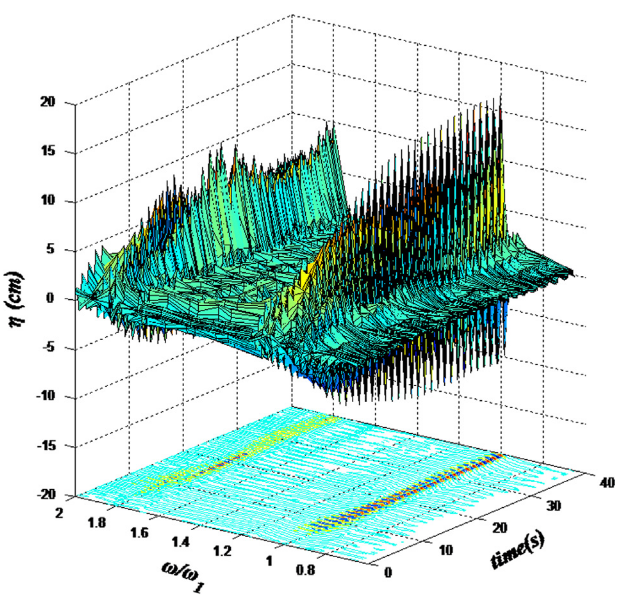

Fig. 6. Time history of the free surface elevations with $a/D=2/3$, $P=0.5$ (case 2 – 1), $A/L=0.0025$ and $D/L=0.5$.

elevation for case 2 – 1 is higher than that for case 1 – 1 (the clean tank), perhaps may be due to the water jet or other non-linear effects. In addition, there is a clear difference between case 10 – 1 and the other cases in Fig. 7, which suggests that the resonant frequency of case 10 – 1 is different from that of the other cases.

Figs. 8 and 9 present the third-order time history of the free surface elevations at different relative submerged depths. In contrast to the first-order mode, significant discrepancies in the maximum free surface elevations appear only when P and a/D are both small (case 10 – 1). In Fig. 8, case 2 – 1 has a minimal influence on the wave surface elevation. In Fig. 9, the maximum free surface elevations do not change significantly, but the period is prolonged for case 4 – 1, i.e., it decreases the resonant frequency. Therefore, for the third-order mode, the plate location and the plate porosity are both important for controlling the sloshing motion. The porosity influences the free surface elevation, and the relative submerged depth changes the period.

3.2. The influence factors of the sloshing free surface elevations

3.2.1. Amplitudes of the non-dimensional free surface elevations at different a/D and P

According to the above-mentioned results, a horizontal perforated plate is useful in restraining free surface elevations. In this section, the effect of the horizontal plate configuration on the sloshing motion is further analyzed.

Figs. 10–12 show the effects of a/D and P on the amplitudes of non-dimensional free surface elevation with an excitation amplitude of $A/L=0.0025$. As shown in Figs. 10–12, the η_{max}/A at $a/D=1/3$ are much smaller values for each porosity. The results indicate that a horizontal perforated plate can effectively reduce the free surface elevations near the first-order resonant frequency, and this reduction is more significant at a smaller relative submerged depth of $a/D=1/3$. An apparent first-order resonant sloshing disappears in case 10 – 1 (in Fig. 12). Figs. 10–12 show that at different relative submerged depths, the η_{max}/A decrease significantly with the decrease in plate porosity in the first-order mode.

However, the η_{max}/A decrease only when a/D and P are both small at the third-order mode. In contrast, the η_{max}/A for a tank with an inner plate may exceed the elevation value of a clean tank if the plate is far from the water surface. Fig. 12 shows that the effect of P becomes distinct when the relative submerged depth nears the water surface, whereas in Figs. 10 and 11, the effect of P is negligible. Additionally, the resonant frequencies are shifted to a lower frequency by the horizontal plate at the third-order mode when the plate's submerged depth is small. All of these findings demonstrate that the relative submerged depth plays a dominant role in the control of the sloshing motion at the third-mode.

Based on the above analysis, a horizontal perforated plate is limited to change the tank resonant frequencies for the first-order or third-order mode. It can restrain first-order sloshing motion and decrease the free surface elevations, but it is effective in reducing the third-order resonant free surface elevations only when $a/D \le 1/3$. Hence, a horizontal perforated plate with $P=0.1$ and $a/D=1/3$ is recommended for suppressing resonant sloshing in a liquid tank.

For all experimental cases, the values of the resonant surface elevations and resonant frequencies are listed in Table 2.

For case 1 – 1 with a clean tank without an inner plate, the non-dimensional resonant frequencies are $\omega/\omega_1=0.996$ (first-order) and $\omega/\omega_1=1.793$ (third-order). These experimental

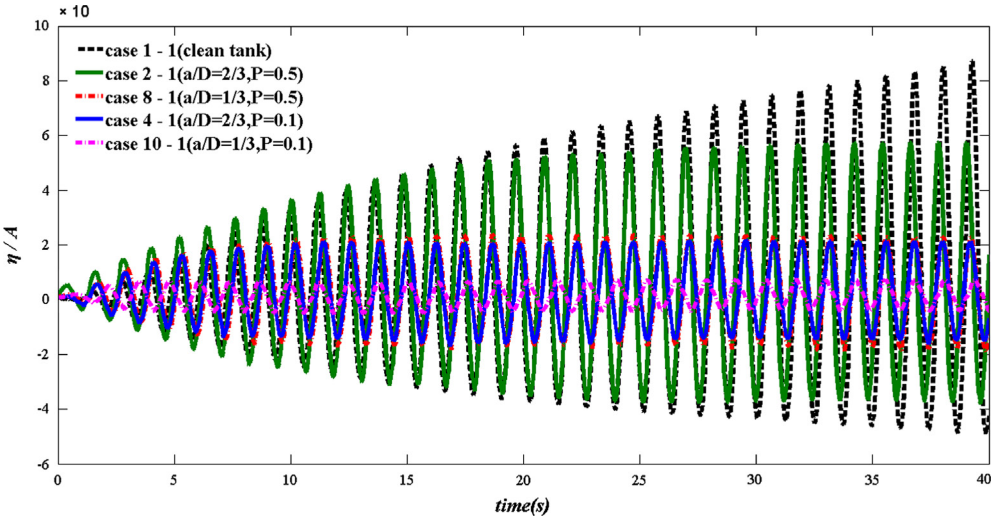

Fig. 7. Time history of the first-order non-dimensional resonant wave surface elevation at $A/L=0.0025$ and $D/L=0.5$ and $\omega/\omega_1=0.996$ (case 1 – 1), 0.996 (case 2 – 1), 0.980 (case 8 – 1), 0.980 (case 4 – 1) and 0.941 (case 10 – 1).

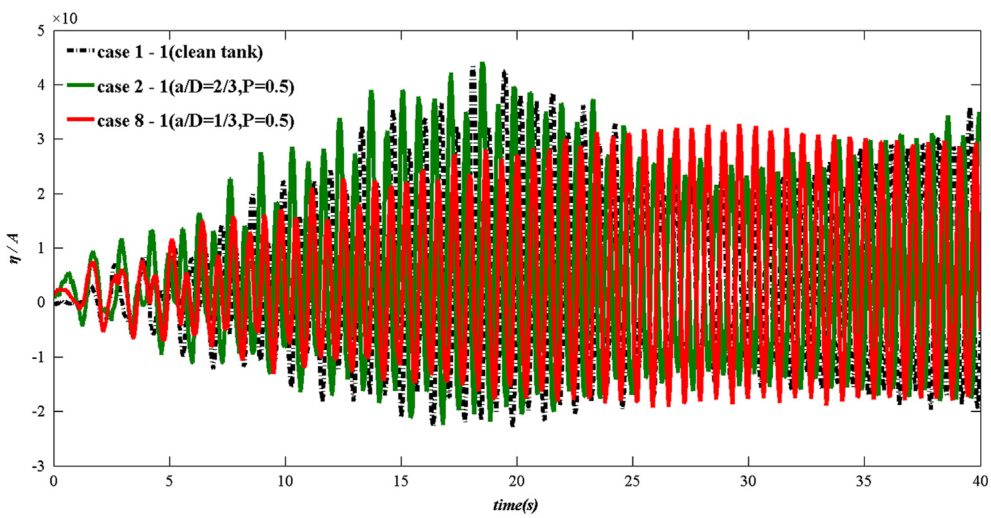

Fig. 8. Time history of the third-order non-dimensional resonant wave surface elevations at $A/L=0.0025$ and $D/L=0.5$ and $\omega/\omega_1=1.793$ (case 1 – 1), 1.790 (case 2 – 1) and 1.773 (case 8 – 1).

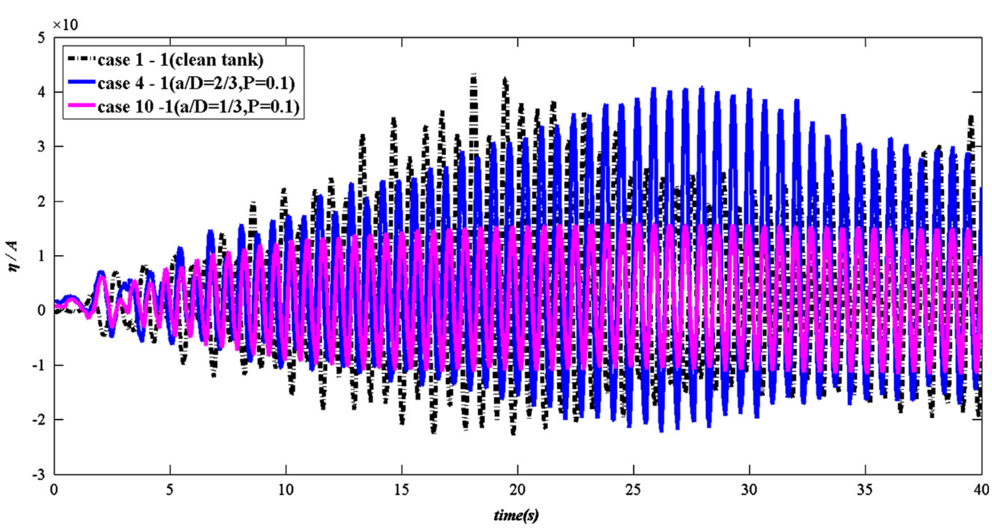

Fig. 9. Time history of the third-order non-dimensional resonant wave surface elevations at $A=2.5$ mm, $D/L=0.5$ and $\omega/\omega_1=1.793$ (case 1 – 1), 1.777 (case 4 – 1), 1.775 (case 10 – 1).

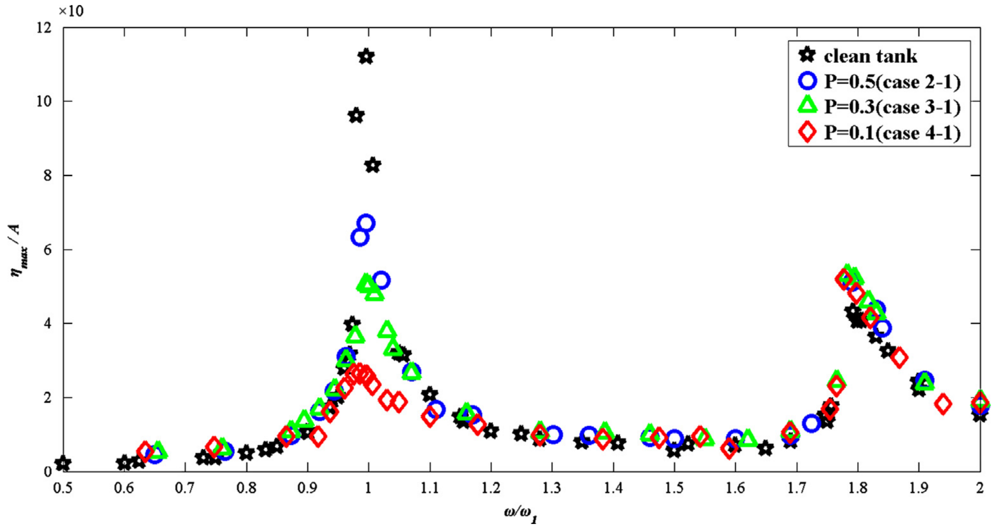

Fig. 10. Amplitudes of the non-dimensional free surface elevations at $a/D=2/3$ and different porosities at $A/L=0.0025$ and $D/L=0.5$.

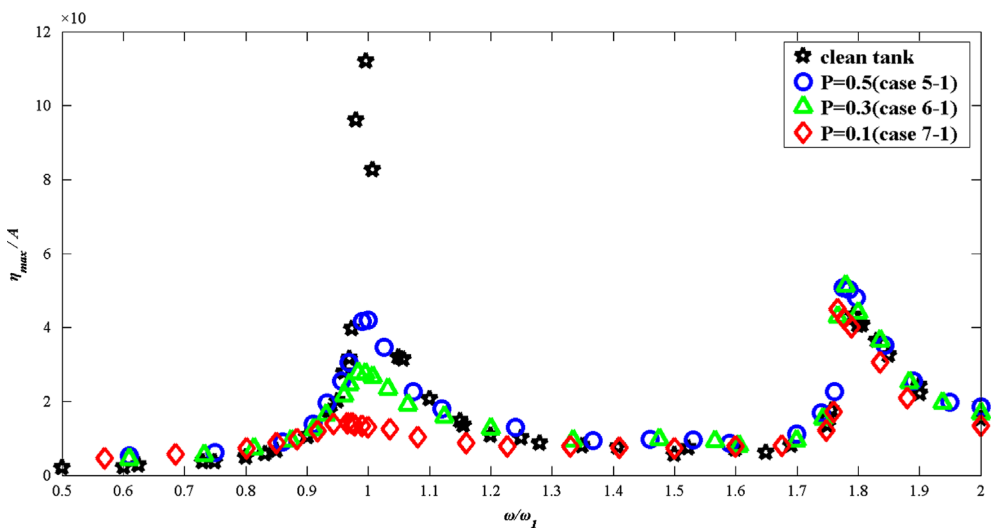

Fig. 11. Amplitudes of the non-dimensional free surface elevations at $a/D=1/2$ and different porosities at $A/L=0.0025$ and $D/L=0.5$.

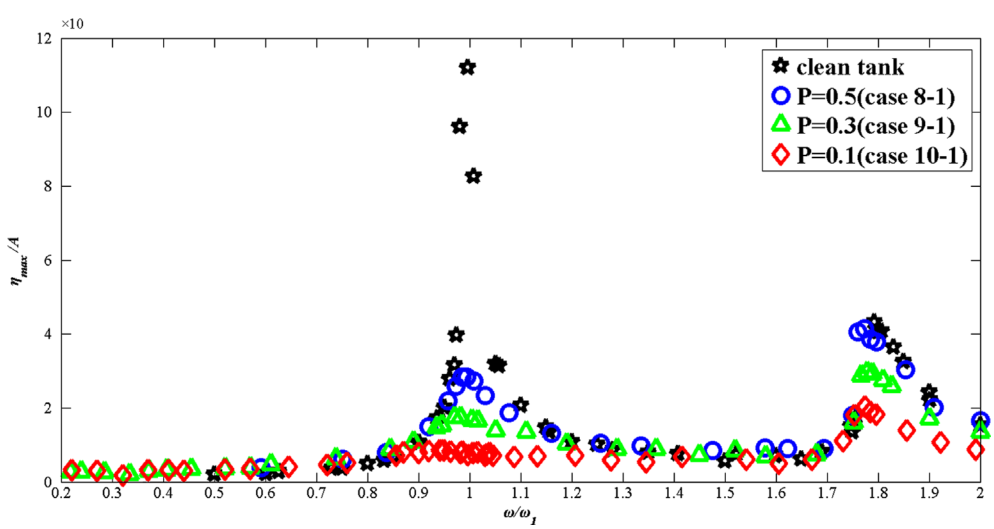

Fig. 12. Amplitudes of the non-dimensional free surface elevations at $a/D=1/3$ and different porosities at $A/L=0.0025$ and $D/L=0.5$.

resonant frequencies ratio are close to the theoretical values of $\omega_1/\omega_1=1$ (first-order) and $\omega_3/\omega_1=1.81$ (third-order). The difference may arise because the experimental data are a number of discrete points and because there are some discrepancies between ideal and experimental conditions (error of measurement, friction and others). Table 2 shows the differences of $\eta_{\max}$ between a clean tank and a tank with an inner plate. The maximum discrepancies are less than 3% (first-order) and 1.5% (third-order). For case 10 – 1, there is no distinct first-order resonant frequency (see in Fig. 12), so we do not list the resonant frequency in Table 2. The result also shows that the variations at the first-order mode tend to diminish away from the natural frequency with a decrease in P and a/D, but limited. However, the effect of the plate on the frequency shows an irregular variation at the third-order mode.

Table 2 shows that the $\eta_{\max}$ are significantly reduced by the horizontal perforated plate. For the first-order mode, the $\eta_{\max}$ decrease monotonously with the decrease in P and a/D. The $\eta_{\max}$ is reduced by approximately 92.4% in case 10 – 1. However, an irregular variation in the $\eta_{\max}$ appears in the third-order mode. The surface elevation shows an obvious variation only for the case in which $a/D=1/3$ and decreases with the decrease in P. The $\eta_{\max}$ of the cases in which the values of a/D are greater than or equal to 1/2 are greater than the free surface elevations in case 1 – 1. These elevations are shown in Figs. 10 and 11. This phenomenon may be explained by the water jet or the reaction of the plate, which needs to be further researched. The minimum $\eta_{\max}$ appear in case 10 – 1 both for the first-order and the third-order modes. This finding indicates that the resonant sloshing at the lower mode can be restrained by a horizontal perforated plate with a small porosity and a small relative submerged depth.

The quantitative analysis indicates that the horizontal perforated plate exerts restriction effect on the sloshing free surface elevations without significantly changing the resonant frequency. The effect of restriction is strong for the first-order mode and limited for the third-order mode.

3.2.2. Amplitudes of the non-dimensional free surface elevations with different excitation amplitudes

Initially, experiments were conducted with a small excitation amplitude, and the same experimental series was then repeated

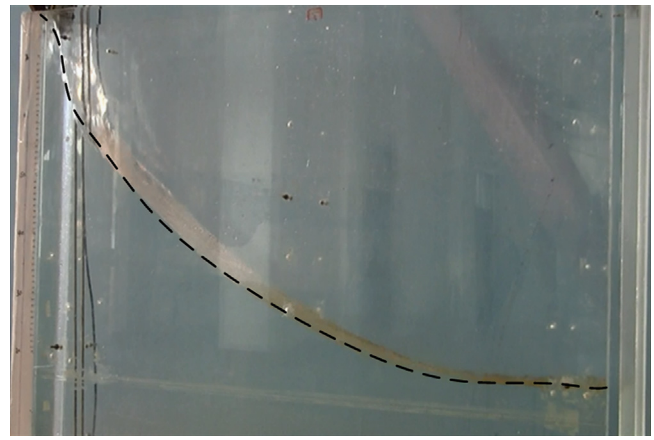

Fig. 14. Snapshot of the sloshing under large-amplitude excitation without the plate.

Table 2
The resonant free surface elevation and resonant frequencies for different plate configurations excited by small-amplitude.

Case	P, a/D	First-order resonant frequency (ω/ω_1)	Free surface elevations (cm)	Third-order resonant frequency (ω/ω_1)	Free surface elevations (cm)
1 – 1	–, –	0.996	28.0	1.793	10.8
2 – 1	0.5, 2/3	0.996	16.8	1.790	12.8
3 – 1	0.3, 2/3	0.996	12.7	1.783	13.3
4 – 1	0.1, 2/3	0.980	6.6	1.777	13.0
5 – 1	0.5, 1/2	1.000	10.5	1.775	12.7
6 – 1	0.3, 1/2	0.986	6.9	1.780	12.9
7 – 1	0.1, 1/2	0.966	3.5	1.767	11.2
8 – 1	0.5, 1/3	0.994	7.1	1.773	10.4
9 – 1	0.3, 1/3	0.982	4.4	1.779	7.4
10 – 1	0.1, 1/3	–	2.1	1.775	5.1

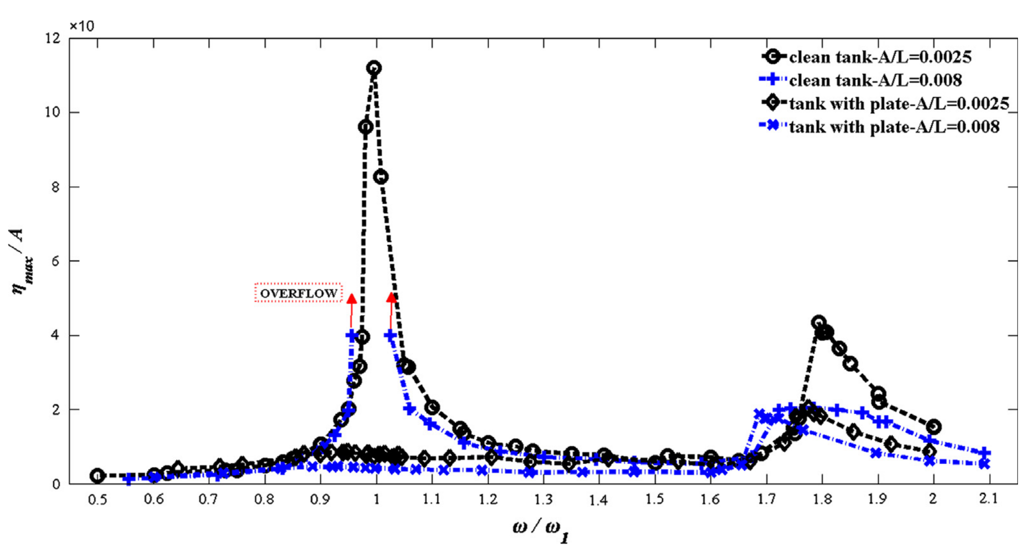

Fig. 13. Comparison of the non-dimensional free surface elevations under different excitation amplitudes at $a/D=1/3$ and $P=0.1$. (For interpretation of the references to color in this figure legend, the reader is referred to the web version of this article.)

with a large-amplitude. Because case 10 – 1 is the best choice for restraining sloshing motion in a tank, a comparison between small and large excitation amplitudes is discussed based on case 10 – 1. The comparison is illustrated in Fig. 13. The red arrow in Fig. 13 indicates that the fluid will continue increasing and will overflow from the tank for the large-amplitude case. Once the η_{max}/A exceeds the limit value, the fluid overflows the tank, and the surface elevation cannot be recorded, as shown in Fig. 14.

Fig. 13 shows the maximum variation in the non-dimensional free surface elevation under different excitation amplitudes. The data for the clean tank under a large excitation amplitude (blue "$- + -$") are missed at the first-order mode, and the value at the third-order mode is also not accurate, whereas the tank with the horizontal perforated plate is successfully captured. The data in the large-amplitude case are missing for two reasons: the η_{max}/A exceeded the upper limit of the tank, and water splash, break and other nonlinear effects prevented data capture. A comparison of the two cases under a large excitation amplitude indicates that the plate is effective for the first-order mode and the resonant sloshing is restrained. The third-order mode shows a complex result, which is caused by nonlinear effects. The observations also show that the η_{max}/A with a large-amplitude is violent and has a large gap compared to the small case. From the curve between $\omega/\omega_1=1.1$ and 1.7, we can see that the large-amplitude magnifies the gap between the cases with and without the perforated plate. Although the maximum free surface elevation at the first-order was not captured, the first-order resonant frequency can be predicted by the trend of the curve. The trend demonstrates that the large-amplitude did not change the non-dimensional frequency, which is in fact similar to that in the small-amplitude case.

3.3. Wave shape

Compared with the free surface elevations measured by the wave probes, the snapshot of the wave shape shows an intuitive characteristic for analyzing the sloshing motion. A standing wave can be observed clearly in Fig. 15. There are two antinodes in Fig. 15b and d, and the wavelength is approximately 2/3 of the tank length. However, the wavelength in Fig. 15a is almost 1/2 of the tank length. The result is similar to that of Faltinsen and Timokha (2009).

Due to the good performance of the horizontal perforated plate, the free surface motion is restrained in Fig. 15c. In contrast with that shown in Fig. 15a and b, the wave shape is much steadier in figures indicating a small submerged depth. Comparing Fig. 15a and b with Fig. 15c and d clearly shows that the wave shape, including the wave antinode locations and the wavelength, are not be influenced by the horizontal perforated plates. The only difference is the significant decrease in the free surface elevations. The effect of the vertical oscillation of water particles in the standing wave, which causes a higher wave amplitude than the first-order resonance, may be the cause of the poor performance of the horizontal perforated plate at the third-order mode. The same phenomenon was observed in the previously discussed analysis of the wave probe data.

The wave shape (Fig. 15a and c) is not that of a rigorous standing wave. There is a linear translation-like wave in this mode.

4. Conclusions

Experimental tests have been conducted to investigate the efficiency and characteristics of a horizontal perforated plate tank system. The effectiveness and characteristics of the tank have been investigated with different horizontal perforated plates under different excitation amplitudes and frequencies. The results of the above study allow for the following conclusions to be drawn.

The horizontal perforated plates are useful in restraining violent sloshing effects in a rectangular tank under horizontal excitation. The characteristics of the tank with a horizontal perforated plate showed that the frequency is minimally influenced by the plates for both first-order and third-order models and that the structure could significantly reduce the wave amplitude. In light of this characteristic, a tank system with horizontal

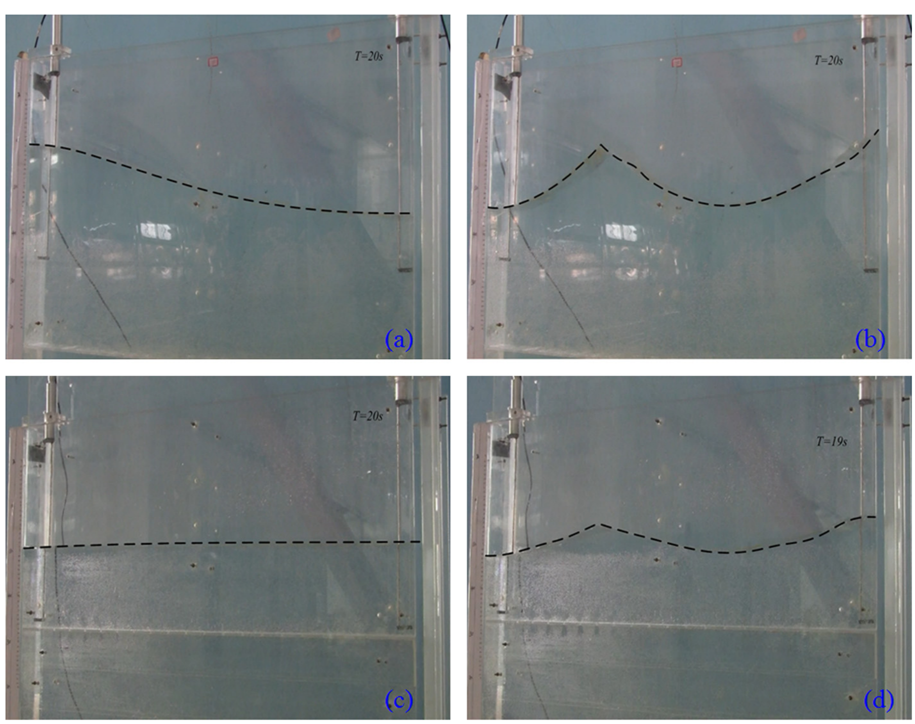

Fig. 15. Resonant wave shape: (a) first-order mode with $P=0.5$ and $a/D=2/3$; (b) third-order mode with $P=0.5$ and $a/D=2/3$; (c) first-order mode with $P=0.1$ and $a/D=1/3$; and (d) third-order mode with $P=0.1$ and $a/D=1/3$.

perforated plates should be considered in designing anti-rolling tanks for ships. The characteristics of this tank system offers a large damping effect to reduce the sloshing wave amplitude, and the structure does not change the frequency, ensuring that the tank's resonant sloshing motion can be activated by the natural frequency and dissipate energy significantly. The first-order resonant frequency for case 10 – 1 cannot be distinguished in Fig. 12. This clearly demonstrates that the perforated plate with $P=0.1$ and $a/D=1/3$ could suppress the resonant wave elevation, significantly. In our experiment series, $P=0.1$ and $a/D=1/3$ is the optimum parameters. Moreover, the general conclusions drawn from this study are as follows: the closer the perforated plate is to the water surface from the bottom, the better the restraining effect it can offer; the plates must be placed under the water surface to ensure proper activity; the total area of the perforations should not exceed 10% to effectively restrain the upward and downward sloshing motion of water between the compartments; and in practice, the P of the plates is due to the strength of the plates and the technical limitations in drilling the slots.

Some details of the sloshing effects observed in the tank with horizontal perforated plates are summarized as follows:

(1) The effect on the $\eta_{\max}/A$ at the third-order mode is small. The elevation shows distinct variation only in the case in which $a/D=1/3$, and the $\eta_{\max}/A$ decrease as P decreases. The $\eta_{\max}/A$ increases and is greater than the clean tank when $a/D=2/3$, $1/2$ at the third-order resonance.
(2) At the beginning of the time history, the free surface elevation of the perforated plate case is higher than that for the clean tank. Several seconds later, the $\eta_{\max}/A$ stop increasing while the $\eta_{\max}/A$ of the clean tank continues to increase and exceed that of the tank with the plate.
(3) The excitation amplitude has a minimal influence on the frequency of the sloshing phenomenon and free surface elevation.
(4) The wave shape for $\omega/\omega_1 < 1.3$ is a linear translation-like wave with a wavelength of approximately $1/2L$. When $1.3 < \omega/\omega_1 < 2$, the wave becomes a standard standing wave, the node moves vertically and the wavelength equals $2/3L$.

Acknowledgments

We would like to thank Dr. Gengshen Liu for his valuable suggestions during the writing of this script. This work was supported by National Basic Research Program of China (Grant no 2011CB013704) and the Natural Science Foundation of China (Grant nos. 51010009 and 51322903).

References

Abramson, H.N., 1966. The dynamic behavior of liquids in moving containers. NASA SP-106, National Aeronautics and Space Administration. Washington, DC.
Akyildiz, H., 2012. A numerical study of the effects of the vertical baffle on liquid sloshing in two-dimensional rectangular tank. J. Sound Vib. 331, 41–52.
Akyildiz, H., Unal, N.E., 2005. Experimental investigation of pressure distribution on a rectangular tank due to the liquid sloshing. Ocean Eng. 32, 1503–1516.
Akyildiz, H., Unal, N.E., 2006. Sloshing in a three-dimensional rectangular tank: numerical simulation and experimental validation. Ocean Eng. 33, 2135–2149.
Armenio, V., Rocca, M.L., 1996. On the analysis of sloshing of water in rectangular containers: numerical study and experimental validation. Ocean Eng. 23, 705–739.
Biswal, K.C., Bhattacharyya, S.K., Sinha, P.K., 2004. Dynamic response analysis of a liquid-filled cylindrical tank with annular baffle. J. Sound Vib. 274, 13–37.
Biswal, K.C., Bhattacharyya, S.K., Sinha, P.K., 2006. Non-linear sloshing in partially liquid filled containers with baffles. Int. J. Numer. Methods Eng. 68, 317–337.
Cassolato, M.R., Love, J.S., Tait, M.J., 2011. Modelling of a tuned liquid damper with inclined damping screens. Struct. Control Health Monit. 18, 674–681.
Cho, J.R., Lee, H.W., Ha, S.Y., 2005. Finite element analysis of resonant sloshing response in a 2D baffled tank. J. Sound Vib. 228 (4–5), 829–845.
Dodge, Franklin T., 2000. The New Dynamic Behavior of Liquids in Moving Containers. Southwest Research Inst, San Antonio, Texas, USA.
Evans, D.V., McIver, P., 1987. Resonant frequencies in a container with a vertical baffle. J. Fluid Mech. 175, 295–307.
Faltinsen, O.M., Firoozkoohi, R., Timokha, A.N., 2010. Analytical modeling of liquid sloshing in a two-dimensional rectangular tank with a slat screen. J. Eng. Math. 70, 93–109.
Faltinsen, O.M., Firoozkoohi, R., Timokha, A.N., 2011. Steady-state liquid sloshing in a rectangular tank with a slat-type screen in the middle: quasilinear modal analysis and experiments. Phys. Fluids 23, 042101.
Faltinsen, O.M., Timokha, A.N., 2009. Sloshing. Cambridge University Press, New York, USA.
Faltinsen, O.M., Timokha, A.N., 2011. Natural sloshing frequencies and modes in a rectangular tank with a slat-type screen. J. Sound Vib. 330, 1490–1503.
Goudarzi, M.A., Sabbagh-Yazdi, S.R., 2012. Analytical and experimental evaluation on the effectiveness of upper mounted baffles with respect to commonly used baffles. Ocean Eng. 42, 205–217.
Isaacson, M., Premasiri, S., 2001. Hydrodynamic damping due to baffles in a rectangular tank. Can. J. Civ. Eng. 28 (4), 608–616.
Jung, J.H., Yoon, H.S., Lee, C.Y., et al., 2012. Effect of the vertical baffle height on the liquid sloshing in a three-dimensional rectangular tank. Ocean Eng. 44, 79–89.
Kim, Y., 2001. Numerical simulation of sloshing flows with impact load. Appl. Ocean Res. 23, 53–62.
Lamb, H., 1932. Hydrodynamics. Cambridge University Press, Cambridge, UK.
Linton, C.M., McIver, P., 2001. Handbook of Mathematical Techniques for Wave/Structure Interactions. Chapman & Hall/CRC, Boca Raton.
Liu, D., Lin, P., 2009. Three-dimensional liquid sloshing in a tank with baffles. Ocean Eng. 36, 202–212.
Liu, Y., Li, Y., 2011. An alternative analytical solution for water-wave motion over a submerged horizontal porous plate. J. Eng. Math. 69, 385–400.
Liu, Y., Li, Y., Teng, B., 2007. Wave interaction with a perforated wall breakwater with a submerged horizontal porous plate. Ocean Eng. 34, 2364–2373.
Panigrahy, P.K., Saha, U.K., Maity, D., 2009. Experimental studies on sloshing behavior due to horizontal movement of liquids in baffled tanks. Ocean Eng. 36, 213–222.
Tait, M.J., El Damatty, A.A., Isyumov, N., 2005a. An investigation of tuned liquid dampers equipped with damping screens under 2D excitation. Earthq. Eng. Struct. Dyn. 34, 719–735.
Tait, M.J., El Damatty, A.A., Isyumov, N., Siddique, M.R., 2005b. Numerical flow models to simulate tuned liquid dampers (TLD) with slat screens. J. Fluids Struct. 20, 1007–1023.
Wu, C.H., Faltinsen, O.M., Chen, B.F., 2013. Time-independent finite difference and ghost cell method to study sloshing liquid in 2D and 3D tanks with internal structures. Commun. Comput. Phys. 13 (3), 780–800.
Xue, M.A., Zheng, J.H., Lin, P.Z., 2012. Numerical simulation of sloshing phenomena in cubic tank with multiple baffles. J. Appl. Math. 21, http://dx.doi.org/10.1155/2012/245702. (Article ID 245702).
Yu, X.P., 2002. Functional performance of a submerged and essentially horizontal plate for offshore wave control: a review. Coast. Eng. J. 44 (2), 127–147.
Yu, X.P., Chwang, A.T., 1994. Water waves above submerged porous plate. J. Eng. Mech., ASCE 120 (6), 1270–1282.